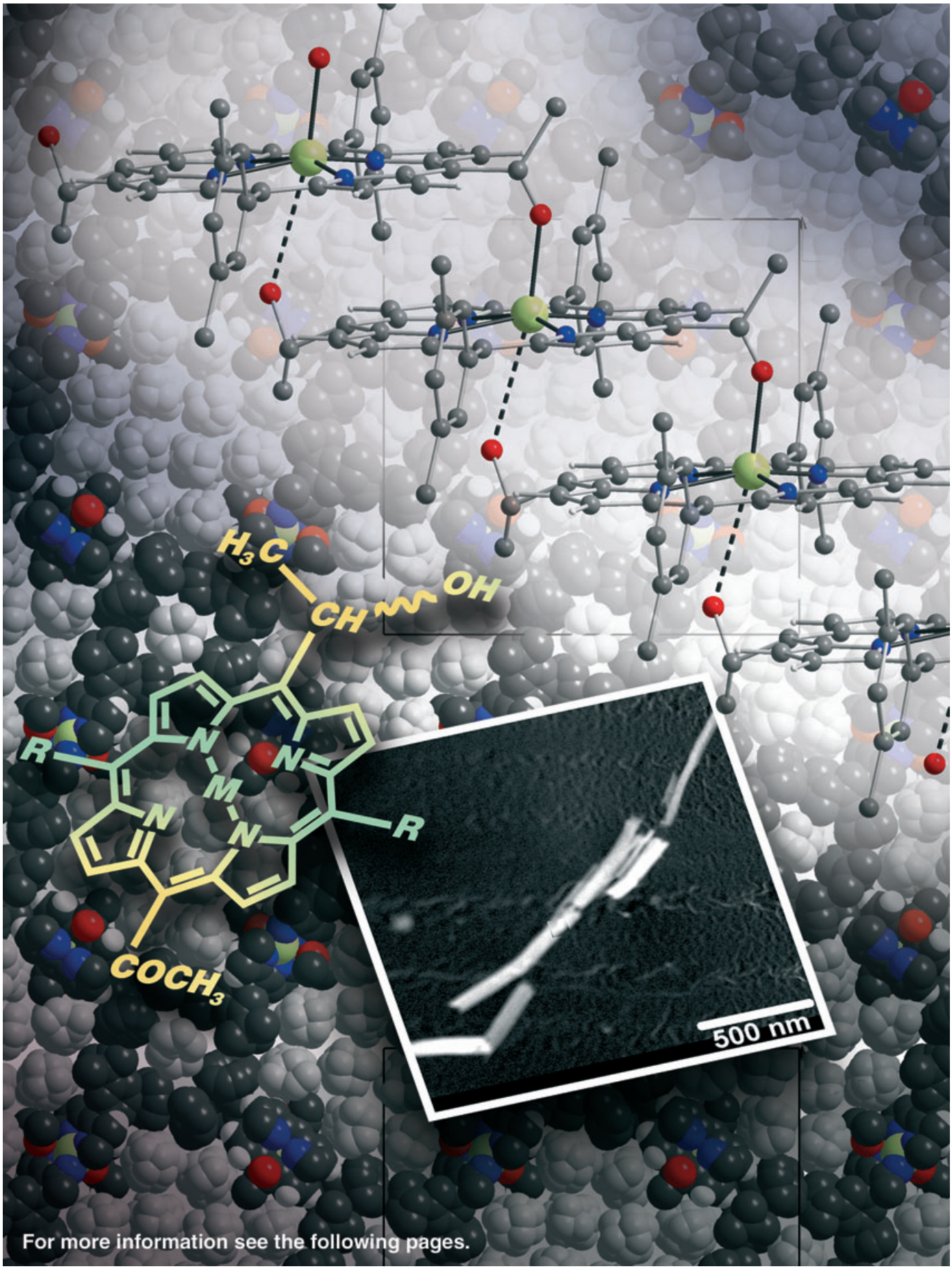

 DOI: 10.1002/chem.200400664

CHEMISTRY
A EUROPEAN JOURNAL

Structural Characterization of Artificial Self-Assembling Porphyrins That Mimic the Natural Chlorosomal Bacteriochlorophylls *c*, *d*, and *e*

Teodor Silviu Balaban,*[a, b] Myriam Linke-Schaetzel,[a, b] Anil D. Bhise,[a] Nicolas Vanthuyne,[c] Christian Roussel,[c] Christopher E. Anson,[d] Gernot Buth,[e] Andreas Eichhöfer,[a] Keir Foster,[a] Győző Garab,[f] Hartmut Gliemann,[a] Richard Goddard,[g] Tamas Javorfi,[f] Annie K. Powell,[b, d] Harald Rösner,[a] and Thomas Schimmel[a, b, h]

Dedicated to Professor Jean-Marie Lehn on the occasion of his 65th birthday

Abstract: We report two crystal structures of a synthetic porphyrin molecule which was programmed for self-assembly. The same groups which ensure that bacteriochlorophylls *c*, *d*, and *e* can self-assemble into the chlorosomal nanorods, the photosynthetic antenna system of some green bacteria, have been engineered into desired positions of the tetrapyrrolic macrocycle. In the case of the 5,15-*meso*-substituted anchoring groups, depending upon the concentration, by using the same crystallization solvents, either a tetragonal or a layered structure of porphyrin stacks were encountered. Surprinsingly, π–π interactions combined with extensive dispersive interactions, which also encompass cyclohexane, one of the crystallization solvents, win over putative hydrogen bonding. We are aware that our compounds differ considerably from the natural bacteriochlorophylls, but based upon our findings, we now question the hydrogen-bonding network, previously proposed to organize stacks of bacteriochlorophylls. Transmission electron microscopy (TEM), atomic force microscopy (AFM), and small-angle X-ray scattering (SAXS) on various isomeric compounds support our challenge of current models for the chlorosomal antenna as these show structures, astonishingly similar to those of chlorosomes.

Keywords: chlorosomes · porphyrinoids · self-assembly · solid-state structures · X-ray diffraction

Introduction

Developments in artificial light-harvesting are currently hampered by a lack of knowledge of the true structural identity of the chlorosome, the unique organelle evolved by green photosynthetic bacteria, which can efficiently capture sunlight, even underwater at depths of over 50 m.[1] The Fenna–Matthews–Olson bacteriochlorophyll *a* (BChl *a*) pro-

[a] Priv. Doz. Dr. T. S. Balaban, Dr. M. Linke-Schaetzel, Dipl.-Chem. A. D. Bhise, Dr. A. Eichhöfer, Dr. K. Foster, Dr. H. Gliemann, Dr. H. Rösner, Prof. Dr. T. Schimmel
Forschungszentrum Karlsruhe
Institute for Nanotechnology, Postfach 3640
76021 Karlsruhe (Germany)
Fax: (+49) 724-782-8298
E-mail: silviu.balaban@int.fzk.de

[b] Priv. Doz. Dr. T. S. Balaban, Dr. M. Linke-Schaetzel, Prof. Dr. A. K. Powell, Prof. Dr. T. Schimmel
Center for Functional Nanostructures
University of Karlsruhe (TH), 76131 Karlsruhe (Germany)

[c] Dr. N. Vanthuyne, Prof. Dr. C. Roussel
Université Aix-Marseille III
UMR: Chirotechnologies: Catalyse et Biocatalyse
Centre de Saint Jerome, 13397 Marseille, CEDEX 20 (France)

[d] Dr. C. E. Anson, Prof. Dr. A. K. Powell
University of Karlsruhe (TH)
Department of Inorganic Chemistry
76131 Karlsruhe (Germany)

[e] Dr. G. Buth
Forschungszentrum Karlsruhe
ANKA-Synchrotron Source, Karlsruhe (Germany)

[f] Dr. G. Garab, Dr. T. Javorfi
Institute of Plant Biology, Biological Research Center
Hungarian Academy of Sciences, Szeged (Hungary)

[g] Dr. R. Goddard
Max-Planck-Institut für Kohlenforschung
Mülheim an der Ruhr (Germany)

[h] Prof. Dr. T. Schimmel
University of Karslruhe (TH)
Institut für Angewandte Physik
76131 Karlsruhe (Germany)

Supporting information for this article is available on the WWW under http://www.chemeurj.org/ or from the author.

DOI: 10.1002/chem.200400664

tein complex, in which radiant energy collected in the chlorosome is trapped, has been crystallized[2] and structurally characterized by X-ray crystallography,[3] but less is known of the chlorosome. Early electron microscopy studies of freeze-fractured chlorosomal samples show a collection of cylindrical rods of 4–5 nm diameter and lengths up to 100 nm or more, enclosed by a monolayer lipid membrane.[4] These nanorods are known to be composed of densely packed chromophores, such as BChls *c*, *d*, or *e* and carotenoids. Although initially subject to considerable debate, it is now generally accepted that the BChls self-assemble into large suprastructures, which exhibit excitation energy transfer without significant self-quenching, even in the absence of interactions with a proteinaceous scaffold. Pigment protein complexes are generally encountered in the antenna systems of purple bacteria,[5] cyanobacteria,[6] or plants.[7] Spectroscopic and microscopic studies have been performed on the chlorosomes and several models for BChl self-assembly have been proposed, based on the interactions between its functional groups.[8] Recently, compelling evidence for the self-assembly of BChls in chlorosomes has been produced by sequencing the entire genome of a green sulfur bacterium,[9] combined with selective gene inactivation studies.[10] In an attempt to mimic the self-assembly ability of BChls *c*, *d*, or *e*, to implement the chlorosomal architectural principle for antenna systems of manmade solar devices, we have synthesized various zinc porphyrins containing the functional groups of the natural system and investigated the supramolecules they tend to form.[11] Here we report two single-crystal X-ray structure analyses of one of the complexes that indicate how the self-assembly in the natural systems may operate. TEM, AFM, confocal fluorescence, and optical microscopy studies on assemblies of isomeric compounds reveal rodlike nanostructures, astonishingly similar to those of the natural case, and the local ordering is documented by SAXS spectra and TEM.

Abstract in French: *Nous présentons ici deux structures cristallographiques d'une porphyrine de synthèse, préprogrammée pour s'auto-assembler. Pour cela, le macrocycle tétrapyrrolique a été doté, sur les positions appropriées, des mêmes groupes fonctionnels que ceux rencontrés dans les chlorosomes, antennes photosynthétiques de certaines bactéries vertes, et qui assurent l'auto-assemblage des bactériochlorophylles* c, d *et* e *en nanotubes. Lorsque ces groupes fonctionnels substituent les positions* méso*-5, 15 du macrocycle, et bien que les mêmes solvants de recristallisation aient été utilisés, deux structures distinctes ont été résolues: les assemblées de porphyrines ont, soit une structure en couche, soit une structure tétragonale en fonction de la concentration. Etonnement, les interactions* π *combinées à des interactions dispersives étendues qui incluent également des molécules de cyclohexane, un des solvants de cristallisation, l'emportent sur des liaisons hydrogène présumées. Nous sommes conscients que nos composés diffèrent énormément des bactériochlorophylles naturelles, mais nos résultats semblent cependant remettre en question le réseau de liaisons hydrogène supposé jusqu'à lors comme l'instigateur de l'assemblage des bactériochlorophylles. Des études par microscopie à transmission électronique (TEM), microscopie à force atomique (AFM) et diffusion à rayons X petit angle (SAXS) réalisées sur nos différents isomères montrent des structures étonnement similaires à ceux rencontrés dans les chlorosomes naturelles, ce qui nous encourage à mettre en débat les modèles courants pour l'empilage de bactériochlorophylles dans les antennes chlorosomales.*

Results and Discussion

Reasoning that self-assembled pigments may have an advantage over other forms of functional antennae,[12] since they can be easily synthesized and follow an organization principle thought to be closest to that of the chlorosome pigments,[8] we have attached the same functional groups that are present in the BChls to selected positions of fully synthetic porphyrins (Figure 1).[11a,b] The starting point was the

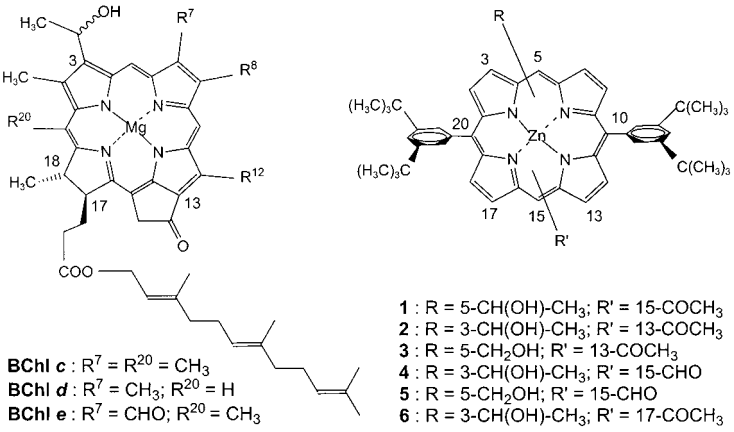

Figure 1. Formulae for the natural BChls (left) and synthetic mimics (right) discussed in this work. R^8 can be a methyl, ethyl, *n*-propyl, or an isobutyl residue. R^{12} can be either a methyl or an ethyl substituent. The fatty alcohol esterifying the 17-propionic acid residue on the left is farnesol; however, stearol, cetol, oleanol, geranyl-geraniol, and phytol are also encountered. For the synthetic mimics an analogy to the (bacterio)chlorophyll numbering is preserved here, so that the hydroxy(m)ethyl substituent (R) is in the northern half (positions 3 or 5) and the carbonyl group in the R′ substituent is in the southern half of the molecule (positions 13, 15, or 17).

synthesis of porphyrins **1**–**6** containing two lipophilic solubility inducing groups (3,5-di-*tert*-butylphenyl) in opposite 10,20-*meso*-positions and two functional groups from BChl. One is a hydroxy(m)ethyl group and the other a carbonyl group (either as formyl, acetyl or longer (C_4–C_{18}) acyl chains).[13] Subsequent zinc metalation of the macrocycles gives molecules that form large self-assembled structures in nonpolar solvents. We chose zinc rather than magnesium, because zinc BChl *a* has been found to be fully functional in a photosynthetic bacterium.[14] Furthermore, these molecules

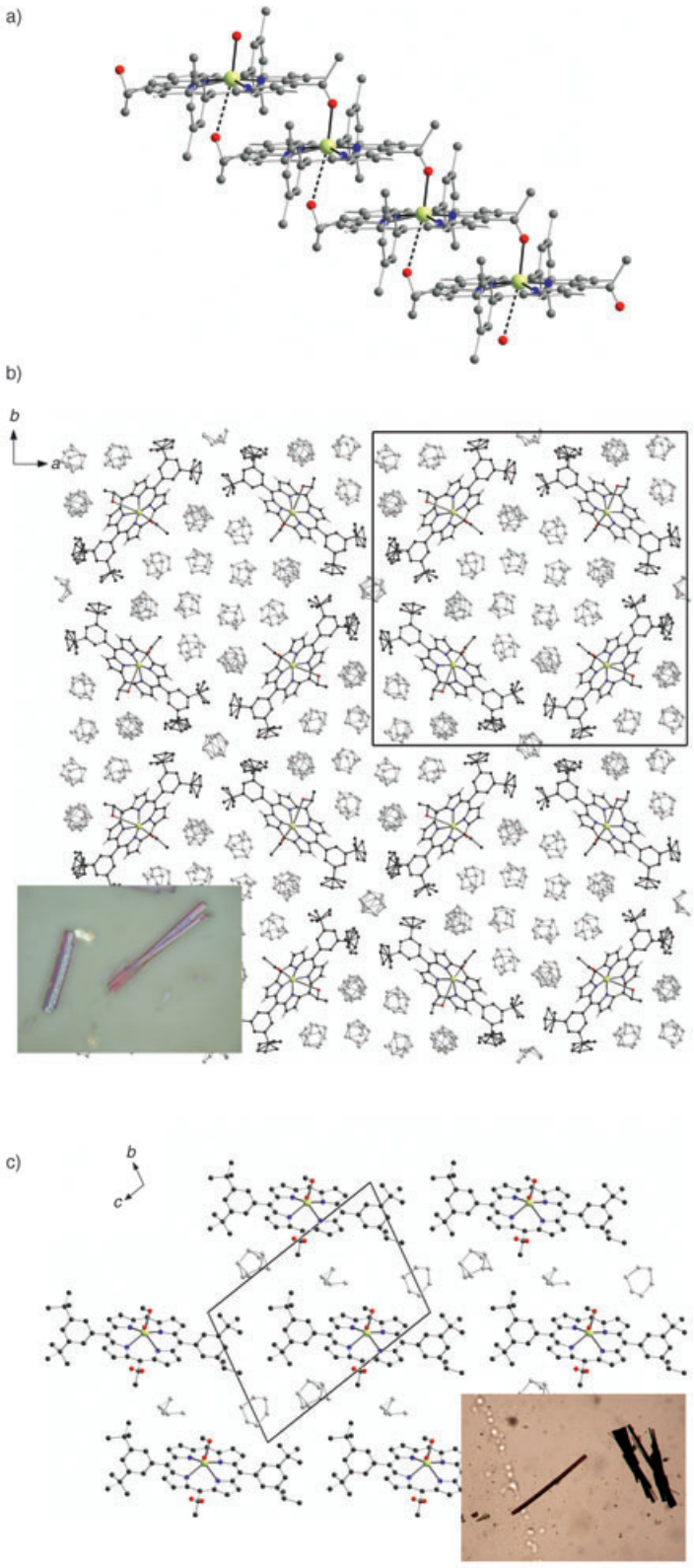

Figure 2. Crystal structure of **1**: zinc green, carbon black, nitrogen blue, and oxygen red. a) Stack of Zn-porphyrins encountered in both crystal modifications, shown here in an upward orientation. Due to statistical disorder, both upward and downward stacks are encountered in the lattice. Long-range carbonyl–zinc interactions are shown with dotted lines. b) Tetragonal packing of the stacks in crystal modification **1A**, which has seven cyclohexane solvent molecules per molecule of **1**, space group $P4_2$. The view is perpendicular to the stacks, along the short *c* crystallographic axis. Inset optical microscopy picture of these crystals. Note that the larger channel between the four stacks is filled with disordered cyclohexane molecules, which are thus are contained within a parallelepiped. Between various parallelepipeds, a smaller channel is filled with a strand of single cyclohexane molecules. For a space filling version of this image see Supporting Information. c) Packing of the stacks in crystal modification **1B**, which has three cyclohexane solvent molecules per molecule **1**, space group $P\bar{1}$. The stacks are cemented together by partially disordered cyclohexane molecules (grey). The view is perpendicular to the stacks, along the short *a* crystallographic axis. Inset optical microscopy picture of these crystals.

are more robust than their natural counterparts and are easily accessible.

Encouragingly, broad absorption spectra are encountered and fluorescence is not quenched when these molecules self-assemble,[11a,b] a fact which is quite untypical for aggregated dyes. This suggests that the porphyrin molecules are arranged in a very orderly manner, and that concentration quenching is not operating. Similarly broad absorption spectra have also been observed by Tamiaki and co-workers, who by using multistep elegant syntheses could induce chlorosomal-type self-assembly in an octaalkylporphyrin.[15] Anhydrous conditions are essential for the self-assembly algorithm to proceed. Methanol competes for zinc ligation and leads to complete disassembly, which can be easily followed by absorption spectra. The broad, red-shifted, aggregate maxima disappear upon addition of stoichiometric excess of methanol due to the formation of the monomeric species.

Crystals of **1** suitable for X-ray diffraction were grown in the absence of other hydroxylic species from a solution of the racemic 10,20-bis(3,5-di-*tert*-butylphenyl)-15-acetyl-5-(1-hydroxyethyl)porphinato zinc in chloroform by slow diffusion of cyclohexane. Depending on the crystallization conditions two different needlelike crystal modifications were encountered. With low chloroform concentrations and very slow cyclohexane diffusion rates tetragonal needles were obtained (modification **1A**), whereas at higher concentrations, smaller and thinner needles formed rapidly which tended to agglomerate (modification **1B**, shown as an inset in Figure 2).

The self-assembled zinc porphyrin complexes have the same extended stack structure in both modifications **1A** and **1B** in spite of significantly different crystal environments, suggesting that ligation of zinc atoms within the porphyrin macrocycle by the oxygen atom of the 1-hydroxyethyl group and extensive π–π stacking of the macrocycles are the dominant interactions (Figure 2). The formation of extended stacks is in accordance with the chlorosomal model proposed by Holzwarth and Schaffner[8i] and indicated on the basis of solid-state MAS ^{13}C NMR data.[8d] Very recently, similar stacks have been postulated in a study of a microcrystalline Cd-BChl *d* analogue by using MAS NMR data together with molecular modelling; based upon intermolecular correlations in the ^{13}C–^{13}C solid-state correlated spectra,

cooperative multiple hydrogen bonding between these stacks was proposed.[8j]

In both **1A** and **1B** the porphyrin rings are parallel with interplanar distances of 3.46 and 3.59 Å, respectively. Within the stacks, the porphyrin rings are inclined such that the respective normals of the mean planes subtend angles of 54.3 and 52.3° to the stack axes. The red-shifted absorption maxima are consistent with the off-set but parallel geometry of the transition dipole moments, as observed in J-aggregates.[16] In both structures, the zinc atoms are disordered above and below the plane of the porphyrin ring, by +0.258 and −0.278 Å (**1A**) and ±0.668 Å (**1B**). Within each stack it is assumed that the zinc atoms are displaced on the same side of the ring plane, but that this intrastack directionality is independent of that in adjacent stacks. Both orientations are present in both modifications in the form of disorder, indicating that the interstack interactions in the crystal have no directional preference. In both structures the acetyl and hydroxyethyl groups are disordered. However, in each case the zinc atoms are displaced towards a disordered oxygen atom (which we assume to be from the hydroxyl group) from the next molecule in the stack, with Zn−O distances Zn1A−O2A″ = 2.204 Å, Zn1B−O1B′ = 2.248 Å in **1A**, and Zn1−O1A′ = 2.37 Å in **1B**.

The most remarkable feature of the structures, however, is the close approach of the carbonyl group of the acetyl moiety of one porphyrin ring to the Zn atom of its neighbor. In both **1A** and **1B** the C=O group occupies a position on the opposite side of the porphyrin to the hydroxyl group, with Zn···O distances Zn1A−O1A″ = 3.528 Å, Zn1B−O2B″ = 3.464 Å in **1A**, and Zn1−O1B″ = 3.70 Å in **1B**. The presumably weak attractive interaction to the carbonyl group to the formally five-coordinate Zn atom is sufficient to cause the acetyl group to twist out of the plane of the porphyrin ring with loss of conjugation with the porphyrin macrocycle, consistent with the purple color of the compound and the $\nu_{C=O}$ stretching frequency at around 1685 cm^{-1}. Interestingly, when a formyl group is in the *meso*-position, it is fully conjugated and leads to a deep green color, even for free-base porphyrins.[11c]

Importantly, there is an absence of any hydrogen bonding between the hydroxyl groups and carbonyl groups, in contradiction to all the current models for the structure of bacteriochlorophylls.[8] Such O−H···O=C hydrogen bonding is not only absent in the crystals **1A** and **1B**, it also does not occur in solutions of **1** in nonpolar solvents. The shift to lower frequencies of the $\nu_{C=O}$ band in the FT-IR spectra of BChl self-assemblies is usually attributed to intermolecular O−H···O=C hydrogen bonding. This hydrogen bonding mode has been proposed to act cooperatively between stacks of BChl molecules[8a–e,i] or both between parallel or antiparallel dimeric BChl assemblies,[8f–h] and is the mostly disputed feature of the self-assembly mechanism.[1] Based on the crystal structures described here, it seems likely that the shift of the $\nu_{C=O}$ band to lower frequencies is not due to hydrogen bonding, but rather to weak carbonyl–metal ligation. Being attached to the metal atom, the carbonyl group is no longer available to act as a hydrogen-bond acceptor. Similarly, the metal–OH ligation provides an explanation for the observed broad and low frequency δ_{O-H} bands, also previously thought to be an indication of O−H···O=C hydrogen bonding. We have recently shown that the hydrogen bonding of a 2-aminopyrimidin-5-yl group attached to a similar porphyrin group can be inhibited due to encapsulation,[17] although it should be noted that the 2-aminopyrimidin-5-yl group does undergo hydrogen bonding in an unrestricted environment.

Interestingly, in both **1A** and **1B** we see no evidence of hydrogen bonding between stacks, although molecular modeling predicts considerable stabilization in the absence of solvent and no severe steric hindrance, in spite of the presence of the two bulky *meso*-3,5-di-*tert*-butylphenyl groups. Clearly, the interstack hydrogen bonding is prevented by either the interaction of the CO group with the zinc atom or cohesive forces between the porphyrin and the surrounding cyclohexane solute, or a combination of both. Presumably, the lipophilic *tert*-butyl groups on the porphyrin ring facilitate interaction with the solute. The weak forces involved and the large number of solute molecules present account for the extreme fragility of the crystals. We are aware that our model systems lack the annulated cyclopentanonic ring that is present in all (B)Chl's and which might prevent, in the case of the natural self-assemblies, the weak metal ligation that must be associated with a twisting of the carbonyl group out of the tetrapyrrolic plane. This five-membered ring is also responsible for the high extinction coefficients of the visible bands in (B)Chl's.[11c]

Table 1. Crystal data and structure refinement summary.

	1A	**1B**
formula	$C_{94}H_{142}N_4O_2Zn$	$C_{70}H_{94}N_4O_2Zn$
M_r	1425.49	1088.86
crystal system	tetragonal	triclinic
space group	$P4_2$	$P\bar{1}$
a [Å]	37.636(3)	5.8521(15)
b [Å]		13.772(4)
c [Å]	5.9561(4)	19.775(5)
α [°]	90	103.65(2)
β [°]	90	92.57(2)
γ [°]	90	98.35(2)
V [Å^3]	8436.5(11)	1527.1(7)
Z	4	1
T [K]	180	150
λ [Å]	0.71073	1.0360
F(000)	3120	588
ρ_{calcd} [Mg m^{-3}]	1.122	1.184
μ [mm^{-1}]	0.340	1.963
data measured	23863	1673
unique data	13858	1216
R_{int}	0.1181	0.0694
observed data [$I > 2\sigma(I)$]	2786	701
$2\theta_{max}$ [°] (resolution [Å])	49.9 (0.83)	48.2 (1.26)
wR_2 (all data)	0.1017	0.3212
S (all data)	0.729	1.119
$R1$ [$I > 2\sigma(I)$]	0.0605	0.1244
parameters/restraints	872/17	192/12
largest diff. peak/hole [e Å^{-3}]	+0.15/−0.16	+0.54/−0.25

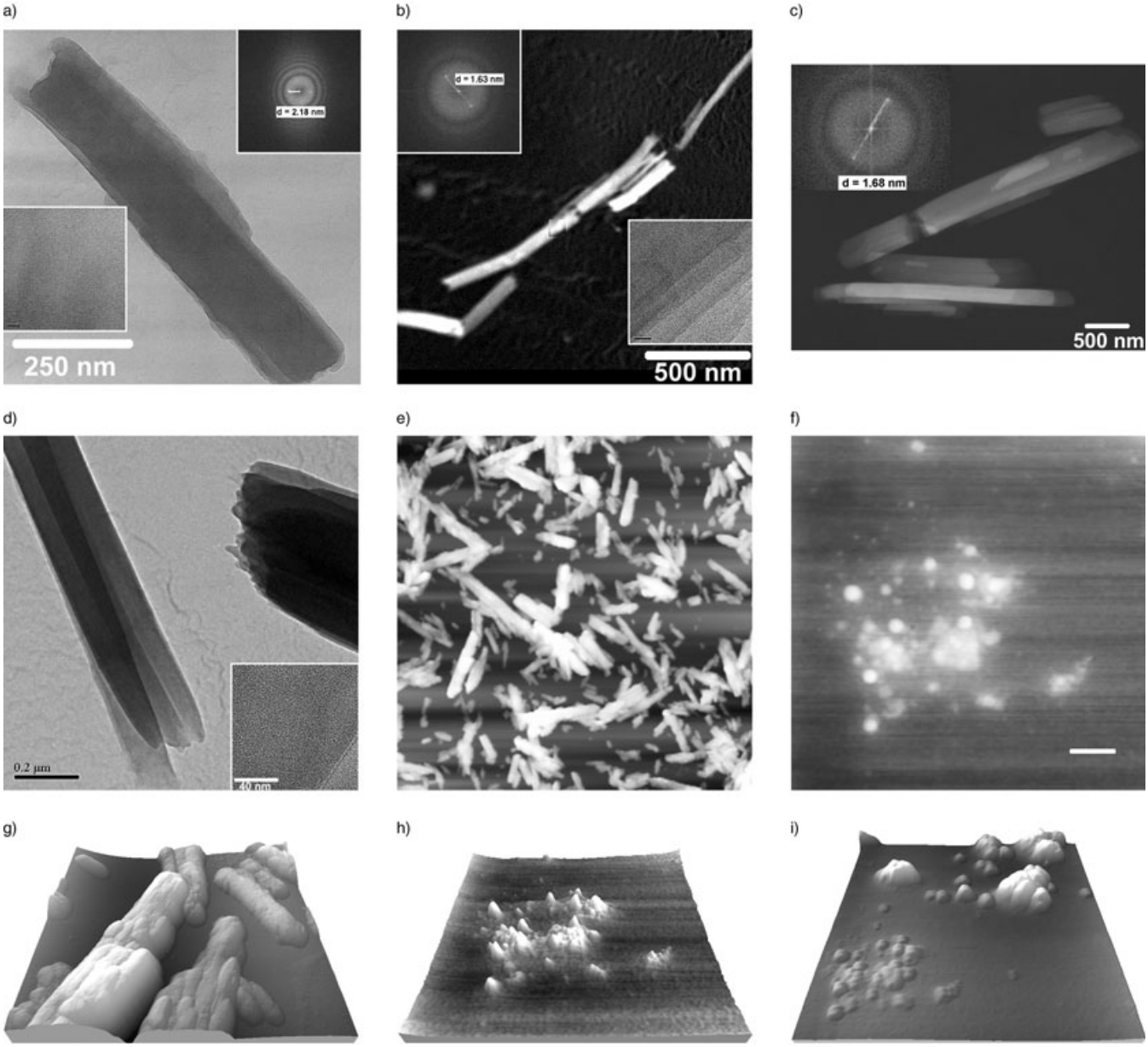

Figure 3. a) TEM bright-field micrograph showing an overview of a rod-like assembly of *rac*-**1**. The inset in the right hand upper corner displays the corresponding diffraction pattern (FFT). Note the diffraction spots which indicate a periodical structure of $d = 2.18$ nm. The propensity of nanotubes is by a factor 100 larger in the racemate samples than with the separated enantiomers. The second inset in the lower right part shows the very faint periodical structure of the assembly (the bar is 20 nm). It is worth noting that these structures disappeared after a few seconds exposure owing to the high dose of electrons (acceleration voltage 200 kV; beam current of about 20 nA). b) STEM micrograph showing an assembly of nanotubes of *rac*-**2**. Note that the *rac*-**2** forms large tubular structures with diameters of about 25 nm and of about 1 μm in length. The inset in the left hand upper corner displays the corresponding diffraction pattern. Note the diffraction spots which indicate a periodical structure of $d = 1.63$ nm. The second inset is a bright-field micrograph showing details and a periodical pattern along the tubular axis of the assemblies (the bar is 40 nm). c) STEM micrograph showing an assembly of nanotubes of *rac*-**6** as an overview. The inset in the right hand upper corner displays the corresponding diffraction pattern. Note the diffraction spots which indicate a periodical structure of $d = 1.68$ nm. d) Bright-field micrograph of *rac*-**6** from dichloromethane/*n*-heptane. Inset: a portion the bright-field micrograph at high magnification. e) AFM overview image of *rac*-**2**. Scan area: 10×10 μm, z range: 300 nm. The sample was prepared on a clean silicon chip by putting one drop of a filtered, solution of *rac*-**2** in dry dichloromethane on the chip and allowing the solvent to evaporate under air. f) AFM image of the achiral **3**. Scan area: 1.5×1.5 μm, z range: 100 nm, scale bar: 300 nm. Sample preparation as above. Note the spherical rather than tubular aspect of the self-assemblies. g) Detail from the image in e), but in topographic representation. Scan size: 1.5×1.5 μm, z range: 700 nm. h) Same AFM image of the achiral **3** as in f), but in a topographic representation. Scan area: 1.5×1.5 μm, z range: 100 nm. i) Topographic AFM image of another portion of **3**. Scan area: 2.5×2.5 μm, z range: 300 nm.

In the structures of both **1A** and **1B** there is statistical disorder of the methyl carbon atom of the 5-(1-hydroxyethyl) group over two positions (50:50) consistent with the presence of a racemic mixture of stereoisomers at the C-5[1] carbon atom in the stack. On the basis of the crystal structure it is not possible to establish whether the disorder is a

result of random racemic variations within individual stacks or superposition of enantiomorphic stacks, though the fact that the crystals were grown from the racemate strongly suggests the former. In support of this, the stacks are straight and we would expect an enantiomorphically pure stack to be helical due to the asymmetry induced by the methyl group. Though this is not the case in **1**, it is worth noting that we have recently shown that in the crystal structures of chlorophyll protein complexes, the diastereoselective coordination of the central magnesium atom has a structural role.[18] In five-coordinate nonsymmetrically substituted tetrapyrroles the central metal atom must therefore be considered as an additional stereocenter. Since the hydroxyl group and the metal atom lie in a bridge that is approximately perpendicular to the plane of the porphyrin ring, the methyl group and the metal atom are each disordered over two positions. Details of the crystallographic analyses are given Experimental Section and in Table 1.

It appears that the formation of extended ordered structures is favored by the presence of both enantiomers. Although (*rac*)-**1** can be conveniently resolved by HPLC on chiral columns,[11a,c] we have as yet not been able to obtain diffraction quality crystals from separated enantiomers, or from **2**–**6**. In addition, rodlike images are obtained by AFM for the racemates of the hydroxylethyl derivatives. Statistical analysis of the images reveals that the propensity to form rods is diminished by two orders of magnitude for the separated enantiomers and that the orderly arrangement evidenced by TEM is entirely absent. Energy dispersive X-ray (EDX) analysis indicates that zinc is present (Supporting Information). Clear regular sheets with 1.6–2.5 nm striations were imaged in several places, depending on the orientation of the rods. Fourier transformation of the diffraction pattern allows a precise estimation of the periodicities (insets in Figure 3 and Supporting Information). The periodicities disappeared after a few seconds exposure due to the high flux of electrons within the TEM beam. These periodic striations appear to arise from parallel stacks of zinc–porphyrin units. Small-angle X-ray scattering (SAXS) data appear to confirm this for compounds **1** and **2**, for which the presence of superstructure peaks indicate periodicities in the two structures with a length scale of 2.10 ± 0.05 and 2.05 ± 0.05 nm, respectively (Figure 4). However, for compound **6** additional peaks are clearly observed. As with samples of **1** and **2**, a strong reflection corresponding to a lattice spacing of 2.1 nm is present, but also an additional peak corresponding to a planar spacing of 1.31 nm is observed, suggesting a different symmetry of this organized phase with respect to those of samples of **1** and **2**. It should be noted, however, that this value is comparable to the *b* lattice constant in **1B**, which is 1.373 nm. Due to the fact that all the SAXS data were collected on powdered samples after prolonged standing under high vacuum, these were solvent free and thus the ordering is expected to be different from the crystal structures which encompass a large amount of cyclohexane, the crystallization solvent that acts like "cement". This might also explain the observed discrepancy between the TEM derived interstack distances (~1.6 nm for compounds **2** and **6**) relative to those obtained from the SAXS profiles (2.05 ± 0.05 nm).

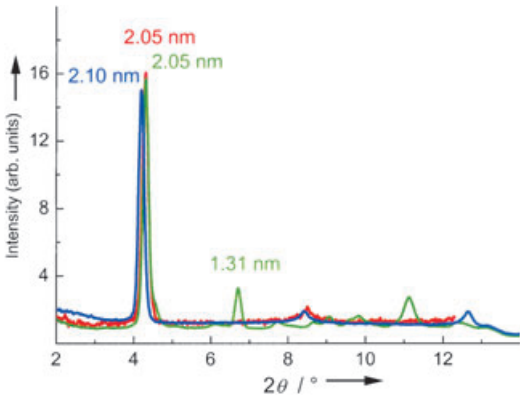

Figure 4. Small angle X-ray scattering (SAXS) spectra. Traces are from samples of the *rac*-**1** (red), *rac*-**2** (blue), and *rac*-**6** (green).

Conclusion

The annulated five-membered ring in the natural (B)Chl's is a structural feature that has been carefully optimized by evolution. It accounts for the increased extinction coefficients of chlorins in the visible region[11c] and forces the 13^1 carbonyl group to be coplanar with the tetrapyrrolic macrocycle. This is not the case with our model compounds in which the carbonyl group in the southern half of the porphyrins is considerably twisted out of conjugation and allows it to approach the zinc atom of the neighboring porphyrin in a stack. Whether this actually happens in the case of the natural magnesium-containing BChls is worth future studies. Presently, we can only state that the mesoscopic behavior, which is due to self-assembly and does not involve hydrogen bonding to this carbonyl group, of several of our model compounds leads to astonishingly similar tubular structures as encountered in the chlorosomal antenna system. After this work was finished and our initial submission of the manuscript, an important study by SAXS and HR-TEM on the natural chlorosomes has been published by Pščenčik et al.,[19] who found a ~2.0 nm spacing very similar to that encountered in several of our compounds (Figures 3 and 4). This fact encourages us to state that our biomimetic approach has been successful and that maybe the current models of the chlorosomal antennas need revision.

One of the long-standing unsolved problems regarding the nature of the chlorosome structure is the question as to why chlorosomes are made up of both stereoisomers of the 3-hydroxylethyl group, whereas nature generally prefers to utilize enantiomerically pure components? Based on these results it is tempting to conclude that a racemic mixture of monomer units leads to linear stacks, which pack more favorably. When the achiral hydroxymethyl substitutent is placed in the porphyrin ring, as in **3** or **5**, spherical assem-

blies with diameters in the 100–500 nm range rather than rods are observed (Figure 3 and Supporting Information), though self-assembly still occurs readily as evidenced by red-shifted absorption (data not shown). Confocal fluorescence and optical microscopy images (data not shown) also allow visualization of the self-assembled species, albeit with much lower resolution. The aggregates are fluorescent, like the chlorosomes, and are thus of potential use as light-harvesting constructs for hybrid solar cells.[11b] Controlling the nature of the self-assembly and interfacing the species with conducting glass electrodes for application as large area solar devices in transparent windows are future challenges. This study provides unprecedented insight into how the self-assembly process of the BChls might operate and opens the way to perfecting artificial antennas for light-harvesting.[11]

Experimental Section

General: The synthesis and characterization of compounds **1**–**6** are given in the Supporting Information of reference [11a] (available on the Internet) and in reference [11c].

X-ray diffraction studies: Data were measured on Stoe IPDS II area detector diffractometers, with graphite-monochromated $Mo_{K\alpha}$ radiation ($\lambda = 0.71073$ Å; **1A**) or Si-monochromated radiation ($\lambda = 1.0360$ Å) on the ANKA-PX beamline for large molecular crystallography of the ANKA synchrotron source at the Forschungszentrum Karlsruhe (**1B**). The beamline optics essentially are composed of a vertically focusing X-ray mirror and a horizontally focusing Si-{111} double-crystal X-ray monochromator (DCM). The Rh-coated silicon X-ray mirror simultaneously acted as a low-pass filter, supressing higher harmonics from the DCM that otherwise would alter the diffraction patterns. For our diffraction studies the DCM was set to a fixed wavelength of 0.1 nm. The actual wavelength and sample–detector distance were calibrated before data collection by recording Debye–Scherrer patterns from a certified X-ray diffraction line position standard (NIST 640c by the National Institute of Standards). Diffraction datasets of the porphyrin crystals were collected on a STOE IPDS II image plate diffraction station and on a Bruker AXS D8 diffractometer equipped with a SMART APEX CCD detector. The sample temperature was kept at 100 K during data collection by means of an Oxford Cryosystems Cryostream cooler. Because of the small size and poor quality of crystals of **1B**, data could only be measured to a resolution of approximately 1.26 Å, but it is still clear from the final structure that the porphyrin stacking is very similar to that in **1A**. Crystal data and refinement details are summarized in Table 1. The structures were solved and refined (full-matrix least-squares against F^2, all data) by using the SHELXTL software suite.[20] In both **1A** and **1B**, the Zn atom was found to be disordered on either side of the plane of the porphyrin ring, with concomitant disorder of the acetyl and hydroxyethyl groups. The cyclohexane molecules were heavily disordered, and were refined using partial carbon atoms. In **1A**, the positions of the Zn atom, the porphyrin ring, and the cyclohexane groups correspond rather closely to the centrosymmetric space group $P4_2/n$. This pseudosymmetry results in a degree of correlation and hence higher-than-expected esds on the structural parameters, preventing unambiguous assignment of the disordered O atoms to the acetyl and hydroxyethyl groups. The structure of **1B** could be refined to a significantly lower wR_2 (0.237 compared to 0.321), in the acentric space group $P1$, but the data/parameter ratio became much too low, and we prefer to accept a higher residual and an adequate ratio in $P\bar{1}$. CCDC-252496 (for **1A**) and CCDC-252497 (for **1B**) contain the supplementary crystallographic data for this paper. These data can be obtained free of charge from The Cambridge Crystallographic Data Centre via www.ccdc.cam.ac.uk/data_request/cif.

Small-angle X-ray scattering (SAXS): The small-angle X-ray scattering (SAXS) measurements were performed on a commercial Bruker Nanostar SAXS system using $Cu_{K\alpha}$ radiation. The system incorporated a gas-filled 2D area detector and a collimation system with pin-hole geometry that produced a low-divergence X-ray beam on the order of 300 microns in diameter. The SAXS samples were prepared by simply allowing a number of drops of solutions of the complexes in dry dichloromethane to evaporate on a thin glass slide (100 μm). Typical measurement times were on the order of 1 h. All measurements were performed in transmission geometry, at room temperature and under a background air pressure of 10^{-3} mbar. The final scattering curves were corrected for background scattering from the sample holder, residual air-scattering and for the detector "dark" current. Measurements were made with a sample–detector distance of 23 cm, providing access to a scattering vector q in the range of $0.65 \le q \le 10\ nm^{-1}$, which would, in principle, allow for the determination of structure sizes D on the order of $0.6 \le D \le 10$ nm.

TEM measurements: TEM specimens were prepared by dropping a suspension of the self-assemblies from either dry dichloromethane or dichloromethane diluted into an excess of dry *n*-heptane onto carbon coated copper grids. Thin films consisting of the remaining solvent and the organic molecules were generated within the Cu grids by this method. The TEM investigations were performed on a Philips Tecnai F20 ST microscope operated at 200 kV with an extraction voltage for the field emission gun of 3.9 keV. The point resolution of this microscope was about 0.235 nm at Scherzer focus and an information limit of about 0.14 nm was obtained. The TEM was equipped with an EDAX energy-dispersive X-ray SiLi detector with a S-UTW (super-ultra-thin window). EDX analyses were carried out in the STEM mode in order to perform nanometre-sized probes (1 nm spot size for the presented EDX measurements). For this purpose an extraction voltage of 4.5 keV was used. Use of a double tilt holder (Gatan) was made. High-resolution micrographs were taken with a 1K×1K CCD camera and analysed with the software package Digital Micrographs (Version 3.5.2, Gatan Company) in order to perform fast Fourier Transformations (FFT).

AFM measurements: For the AFM investigations 10×10 mm pieces of a silicon wafer (Si-100, polished, Wacker, Germany) were treated with Piranha solution (H_2SO_4 (conc.)/H_2O_2 (30%) 4:1) for 10 min, rinsed with water and dried under nitrogen. Then a drop of the porphyrin dissolved in dry dichloromethane was put on the silicon substrate and dried in air.

All AFM investigations were carried out with a Multimode AFM system combined with a Nanoscope IIIa controller (Digital Instruments, USA), which was operated in the intermittent contact mode. Bar-shaped Si_3N_4 cantilevers (Silicon-MDT, Russia) with a typical spring constant of $7.5\ N\,m^{-1}$ were used for **3**, while bar-shaped Si cantilevers (spring constant: $0.6\ N\,m^{-1}$) were used for rac-**2**.

Acknowledgements

Part of this research was supported by the Deutsche Forschungsgemeinschaft through projects C3.2 and C3.6. of the Center for Functional Nanostructures at the University of Karlsruhe.

[1] "Light-harvesting Nanostructures": T. S. Balaban, in *Encyclopedia of Nanoscience and Nanotechnology, Vol. 4* (Ed.: H. S. Nalwa), American Scientific, Los Angeles, **2004**, pp. 505–559.
[2] J. M. Olson, in *The Photosynthetic Bacteria* (Eds.: R. K. Clayton, W. R. Sistrom), Plenum, New York, **1978**.
[3] a) R. E. Fenna, B. W. Matthews, *Nature* **1975**, *258*, 573–577; b) for a more recent structure, see A. Camara-Artigas, R. E. Blankenship, J. P. Allen, *Photosynth. Res.* **2003**, *75*, 49–55.
[4] a) L. A. Staehelin, J. R. Golecki, R. C. Fuller, G. Drews, *Arch. Microbiol.* **1978**, *119*, 269–277; b) L. A. Staehelin, J. R. Golecki, G. Drews, *Biochim. Biophys. Acta* **1980**, *589*, 30–45.
[5] a) G. McDermott, S. M. Prince, A. A. Freer, A. M. Hawthornthwaite-Lawless, M. Z. Papiz, R. J. Cogdell, N. W. Isaacs,

Nature **1995**, *374*, 517–521; b) J. Koepke, X. Hu, C. Muenke, K. Schulten, H. Michel, *Structure* **1996**, *4*, 581–597; c) A. W. Roszak, T. D. Howard, J. Southall, A. T. Gardiner, C. J. Law, N. W. Isaacs, R. J. Cogdell, *Science* **2003**, *302*, 1969–1972.

[6] a) A. Zouni, H.-T. Witt, J. Kern, P. Fromme, N. Krauss, W. Saenger, P. Orth, *Nature* **2001**, *409*, 739–743; b) K. N. Ferreira, T. M. Iverson, K, Maghlaoui, J. Barber, S. Iwata, *Science* **2004**, *303*, 1831–1838; c) P. Jordan, P. Fromme, H.-T. Witt, O. Klukas, W. Saenger, N. Krauss, *Nature* **2001**, *411*, 909–917.

[7] a) W. Kühlbrandt, D. N. Wang, Y. Fujiyoshi, *Nature* **1994**, ***367***, 614–621; b) Z. Liu, H. Yan, K. Wang, T, Kuang, J. Zhang, L. Gui, X. An, W. Chang, *Nature* **2004**, *428*, 287–292; c) A. Ben-Shem, F. Frolow, N. Nelson, *Nature* **2003**, *426*, 630–635.

[8] a) D. C. Brune, T. Nozawa, R. E. Blankenship, *Biochemistry* **1987**, *26*, 8644–8652; b) R. E. Blankenship, J. M. Olson, M. Miller, in *Anoxygenic Photosynthetic Bacteria* (Eds.: R. E. Blankenship, M. T. Madigan, C. E. Bauer), Kluwer Academic, **1995**, pp. 399–435; c) P. Hildebrandt, K. Griebenow, A. R. Holzwarth, K. Schaffner, *Z. Naturforsch. C* **1991**, *46*, 228–232; d) T. S. Balaban, A. R. Holzwarth, K. Schaffner, G.-J. Boender, H. J. M. de Groot, *Biochemistry* **1995**, *34*, 15259–15266; e) J. Chiefari, K. Griebenow, F. Fages, N. Griebenow, T. S. Balaban, A. R. Holzwarth, K. Schaffner, *J. Phys. Chem.* **1995**, *99*, 1357–1365; f) Z.-Y. Wang, M. Umetsu, K. Yoza, M. Kobayashi, M. Imai, Y. Matsushita, N. Niimura, T. Nozawa, *Biochim. Biophys. Acta* **1997**, *1320* 73–82; g) Z.-Y. Wang, M. Umetsu, M. Kobayashi, T. Nozawa, *J. Am. Chem. Soc.* **1999**, *121*, 9363–9369; h) Q.-M. Xu, L.-J. Wan, S.-X. Yin, C. Wang, C.-L. Bai, T. Ishii, K. Uehara, Z.-Y. Wang, T. Nozawa, *J. Phys. Chem. B.* **2002**, *106* 3037–3040; i) A. R. Holzwarth, K. Schaffner, *Photosynth. Res.* **1994**, *41*, 225–233; i) B. J. van Rossum, D. B. Steensgaard, F. M. Mulder, G.-J. Boender, A. R. Holzwarth, K. Schaffner, H. J. M. de Groot, *Biochemistry* **2001**, *40*, 1587–1595; j) I. de Boer, J. Matysik, M. Amakawa, S. Yagai, H. Tamiaki, A. R. Holzwarth, H. J. M. de Groot, *J. Am. Chem. Soc.* **2003**, *125* 13374–13375.

[9] J. A. Eisen, K. E. Nelson, I. T. Paulsen, J. F. Heidelberg, M. Wu, R. J. Dodson, R. Deboy, M. L. Gwinn, W. C. Nelson, D. H. Haft, E. K. Hickey, J. D. Peterson, A. S. Durkin, J. L. Kolonay, F. Yang, I. Holt, L. A. Umayam, T. Mason, M. Brenner, T. P. Shea, D. Parksey, W. C. Nierman, T. V. Feldblyum, C. L. Hansen, M. B. Craven, D. Radune, J. Vamathevan, H. Khouri, O. White, T. M. Gruber, K. A. Ketchum, J. C. Venter, H. Tettelin, D. A. Bryant, C. M. Fraser, *Proc. Natl. Acad. Sci. USA* **2002**, *99*, 9509–9514.

[10] N. U. Frigaard, A. G. M. Chew, H. Li, J. A. Maresca, D. A. Bryant, *Photosynth. Res.* **2003**, *78*, 93–117.

[11] a) T. S. Balaban, A. D. Bhise, M. Fisher, M. Linke-Schaetzel, C. Roussel, N. Vanthuyne, *Angew. Chem.* **2003**, *115*, 2190–2194; *Angew. Chem. Int. Ed.* **2003**, *42*, 2140–2144; b) M. Linke-Schaetzel, A. D. Bhise, H. Gliemann, T. Koch, T. Schimmel, T. S. Balaban, *Thin Solid Films* **2004**, *451–452*, 16–21; c) T. S. Balaban, M. Linke-Schaetzel, A. D. Bhise, N. Vanthuyne, C. Roussel, *Eur. J. Org. Chem.* **2004**, 3919–3930.

[12] S. Hecht, J. M. J. Fréchet, *Angew. Chem.* **2001**, *113*, 76–94; *Angew. Chem. Int. Ed.* **2001**, *40*, 74–91.

[13] Full experimental details on the synthetic procedures are partially available[11a] and are given elsewhere.[11c]

[14] N. Wakao, N. Yokoi, N. Isoyama, A. Hiraishi, K. Shimada, M. Kobayashi, H. Kise, M. Iwaki, S. Itoh, S. Takaichi, Y. Sakurai, *Plant Cell Physiol.* **1996**, *37*, 889–893.

[15] H. Tamiaki, S. Kimura, T. Kimura, *Tetrahedron* **2003**, *59*, 7423–7435.

[16] a) D. Möbius, *Adv. Mater.* **1995**, *7*, 437–444; b) A. Mishra, R. K. Behera, P. K. Behera, B. K. Mishra, G. M. Behera, *Chem. Rev.* **2000**, *100*, 1973–2012.

[17] T. S. Balaban, R. Goddard, M. Linke-Schaetzel, J.-M. Lehn, *J. Am. Chem. Soc.* **2003**, *125*, 4233–4239.

[18] a) T. S. Balaban, P. Fromme, A. R. Holzwarth, N. Krauß, V. I. Prokhorenko, *Biochim. Biophys. Acta* **2002**, *1556*, 197–207; b) T. S. Balaban, *FEBS Lett.* **2003**, *545*, 97–102; Erratum: *FEBS Lett.* **2003**, *547*, 235; c) T. S. Balaban, *Photosynth. Res.* in press.

[19] J. Pščenčik, T. P. Ikonen, P. Laurinmäki, M. C. Merckel, S. J. Butcher, R. E. Serimaa, R. Tuma, *Biophys. J.* **2004**, *87*, 1165–1172.

[20] G. M. Sheldrick, SHELXTL 5.1, Bruker AXS Inc., 6300 Enterprise Lane, Madison, WI 53719-1173 (USA) **1997**.

Received: May 20, 2004
Revised: October 19, 2004
Published online: January 5, 2005

